Computational Intelligence in Electrical Engineering
Vol. 12, No. 4, 2022
Research Paper

Dynamic Stability Improvement in Power System with Simultaneously and Coordinated Control of DFIG and UPFC

Masoud Maleki Rizi[1], Saeed Abazari[2], Nima Mahdian[3]

[1] Ph.D. Student, Department of Engineering, Faculty of Electrical Engineering, Shahrekord University, Shahrekord, Iran
masoud_maleki@yahoo.com
[2] Associate Prof., Department of Engineering, Faculty of Electrical Engineering, Shahrekord University, Shahrekord, Iran
Abazari-s@eng.sku.ac.ir
[3] Assistant Prof., Shahid Rajaei Teacher Training University, Tehran, Iran
nimamahdian@sru.ac.ir

Abstract :
This paper presents the impact of simultaneous and coordinated control of the unified power flow controller (UPFC) and the doubly-fed induction generator (DFIG) on the multi-machine power system`s dynamic stability. All UPFC`s main basic PI controllers and its Power Oscillation Damping (POD) supplementary controller have been used. A more complete model of DFIG and both Rotor-Side Converter (RSC) and Grid-Side Converter (GSC) dynamics with their PI controllers are considered, too. UPFC and DFIG controllers are simultaneously coordinated and optimized with compromising between their control variables parameters. Particle Swarm Optimization (PSO) algorithm is used to optimize the objective function based on eigenvalues and damping ratio to reach the best parameters and variables of controllers of both UPFC and DFIG. During the studies of permanent and dynamic state, the thermal capacity of the lines and the nominal values of UPFC have also been considered. Simulation results in a *39-bus 10-machine New-England power system* show the capability of the applied method. The results demonstrate that coordinated control of UPFC and DFIG tend to more damping system modes oscillation and more stability in the power system.

Keywords: Doubly-fed induction generator, dynamic stability, multi-machine power system, optimization, unified power flow controller.

1. Introduction

Unified power flow controller (UPFC) is an effective flexible alternating current transmission system (FACTS) device that helps overcome some of existing power system operation limitations. It is the most important and comprehensive device that helps stability improvement in power systems. UPFC is equipped with a power oscillation damping (POD) and the damping effect of this POD is better than the power system stabilizer (PSS).

On the other hand, renewable resources based energy conversion systems and in particular wind energy conversion systems (WECS) are growing fast due to environmental issues and natural resources limitations. Application of wind energy to produce electrical energy using doubly-fed induction generators

[1] Submission date:24, 01, 2021
Acceptance date: 08, 08, 2021
Corresponding author: Saeed Abazari, Associate Prof., Department of Engineering, Faculty of Electrical Engineering, Shahrekord University, Shahrekord, Iran

http://dx.doi.org/10.22108/isee.2021.127138.1448

(DFIGs) is growing in power systems because DFIGs allows a large portion of the wind energy to be absorbed. The interaction of DFIG controllers will occur with both electrical and mechanical system modes leading to electrical and mechanical oscillations [1].

The stability enhancement of three-machine system using the coordinated application of the UPFC and the PSS designed employing the Firefly algorithm was already compared with Genetic search algorithm approach [2]. UPFC POD controller design in MMPS, in three-machine system, with selecting damping ratio based objective function linear quadratic regulation (LQR) was used under different loading condition and better result demonstrated [3]. The improved grey wolf optimizer (IGWO) was compared with the differential evolution (DE) and particle swarm optimization (PSO) to optimize UPFC POD controller with integral of time-weighted absolute error (ITAE) criteria and the results demonstrated the stability enhancement of MMPS in three-machine system while comparing using either m_B or δ_E [4].

The effect of DFIG controllers and system parameters in linear modal analysis of DFIG torsional interaction was investigated and the results showed that the DFIG controllers should be adjusted, otherwise, an interaction may occur and the system oscillations increases, and even it becomes unstable. Comparison analysis on damping mechanisms of power systems with induction generator-based wind power generation have done by Bu in multi machine power system and model with RSC dynamics and without RSC dynamics model with fixed rotor speed and with offset rotor voltage only and with constant rotor voltage were studied [5].

Today, many power systems consist of DFIG based wind energy conversion systems because of their economic and environmental advantages and using UPFC because of its operational and economical capabilities. Beside their main advantages they have interactions and influence the stability of power system. So, many new studies have focused on effects of each of these two devices on the other device or the overall power system.

UPFC can be used to improve the overall performance of wind energy conversion system (WECS) through the development of an appropriate control algorithm. The application of a UPFC control algorithm is also investigated in a research to overcome some problems associated with the internal faults associated with WECS [6]. UPFC controller mitigates the harmonic distortion that caused by nonlinear loads. Wind power generation with DFIG provides good performance for terminal voltage recovery after fault clearance owing to its ability to control reactive power however DFIG is sensitive to severe voltage dips [7]. The simulation results show that UPFC can improve the low voltage ride through (LVRT) of DFIG-based WECS and finally maintain wind turbine connection to the grid during certain levels of voltage fluctuation at the grid side [8]. UPFC can satisfactorily improve the LVRT limitation of DFIG-based wind energy source in fault condition [9]. UPFC is used to improving the LVRT of WECS and oscillations of induction generator under fault conditions. Also, it can improve the voltage at the PCC in the fault period [10]. UPFC can significantly improve the Fault ride through (FRT) capability of WECS, so it can support the grid during fault conditions [11]. UPFC has been used in a DFIG based wind turbine system to provide dynamic reactive power support at the PCC in the occurrence of three-phase fault condition [12]. In a transient stability study, a control proposed for the admittance model of the UPFC has validated in a DFIG wind farm penetrated a two-area four-machine power system. The power output of the DFIG was stabilized which helped to maintain the equilibrium between the electrical and mechanical power of the nearby generators. Subsequently the rotor angular deviation of the respective generators gets recovered, which significantly stabilized the network [13]. Performance of wind power and UPFC to increase the fault critical clearing time of power system using MATLAB/SIMULINK software investigated by simulation of IEEE 3 machines 9 buses and showed that the better result will be obtained while these two devices are in the optimum location [14].

Then, due to increasing in penetration level of wind power in large power system may equipped with UPFC, it is important to study and improve this stability in the large multi machine power systems in which both UPFC and DFIG are installed. Then, we have studied more complete small signal models of UPFC and DFIG to investigate the damping effects of UPFC and DFIG in multi machine power systems, considering all dynamic states of both of them in comparison with previous studies. We have considered practical constraints too while using PSO to optimize the control parameters of them. PSO detail algorithm can be found in [15]. In the following sections UPFC and its small signal model and control aspects of it are introduced. Then DFIG small signal modeling and control are reviewed. Models and used optimization algorithm are described. In the last section the simulation results of these two devices individually and together application in dynamic stability are demonstrated and compared.

2. Unified power flow controller

As is seen in figure 1, UPFC consists of two converters coupled through a common DC link. Equation (1) expresses the UPFC terminals voltages.

$$\bar{V}_E = \frac{m_E Vdc}{2} e^{j\delta_E}, \bar{V}_B = \frac{m_B Vdc}{2} e^{j\delta_B} \quad (1)$$

Where:

m_B is the pulse width modulation of series(boosting) inverter. m_E is the pulse width modulation of shunt (exciting) inverter. δ_B is the phase angle of series injected voltage. δ_E is the voltage phase angle of the shunt inverter.

The series branch of the UPFC injects an AC voltage with controllable magnitude and phase angle at the power frequency. Then it can exchange real and reactive power with installed line. The shunt converter is primarily used to provide active power demand of the series converter through a common DC link and can exchange reactive power to adjust the voltage of the bus, which is connected. So, due to these capabilities, UPFC is excellent choice for damping power system oscillations. This damping can be obtained by regulating the controllable abovementioned parameters by controlling decoupled variables of the UPFC by the following four controllers:

$$\delta_B = \left(\frac{1}{1+T_{\delta B}s}\right)\left(K_{Pp}+\frac{K_{Pi}}{s}\right)(P_{Ref}-P) \quad (2)$$

$$m_B = \left(\frac{1}{1+T_{mB}s}\right)\left(K_{Qp}+\frac{K_{Qi}}{s}\right)(Q_{Ref}-Q) \quad (3)$$

$$m_E = \left(\frac{1}{1+T_{mE}s}\right)\left(K_{Vp}+\frac{K_{Vi}}{s}\right)(V_{Ref}-V) \quad (4)$$

$$\delta_E = \left(\frac{1}{1+T_{\delta E}s}\right)\left(K_{DCp}+\frac{K_{DCi}}{s}\right)(V_{DC,Ref}-V_{DC}) \quad (5)$$

Where:

T_x are delay time constants, and K_{xp} and K_{xi} are PI controllers proportional and integral gains respectively. P, Q, V and V_{DC} are flowing active, reactive power through line, bus voltage in which UPFC is connected and UPFC dc link voltage respectively.

The comprehensive models of UPFC for steady-state, transient stability and dynamic stability studies and also a dynamic model of the system installed with UPFC have presented in [16, 17]. A unified model of a multi-machine power system and developed UPFC models is proposed that has been linearized and incorporated into the Heffron-Phillips model [17]. The conflict between these four UPFC multiple control functions and their interactions was investigated and it is showed that sometimes application of all four control function may decrease the accuracy of the results [18]. We used all of these four controllers simultaneously and made a compromise between four control variables. Due to technical and economical restriction the rating of the UPFC power is limited and this leads to applying limits of its real and reactive power by additional limiter blocks and then modifying the UPFC related parameters in each iteration.

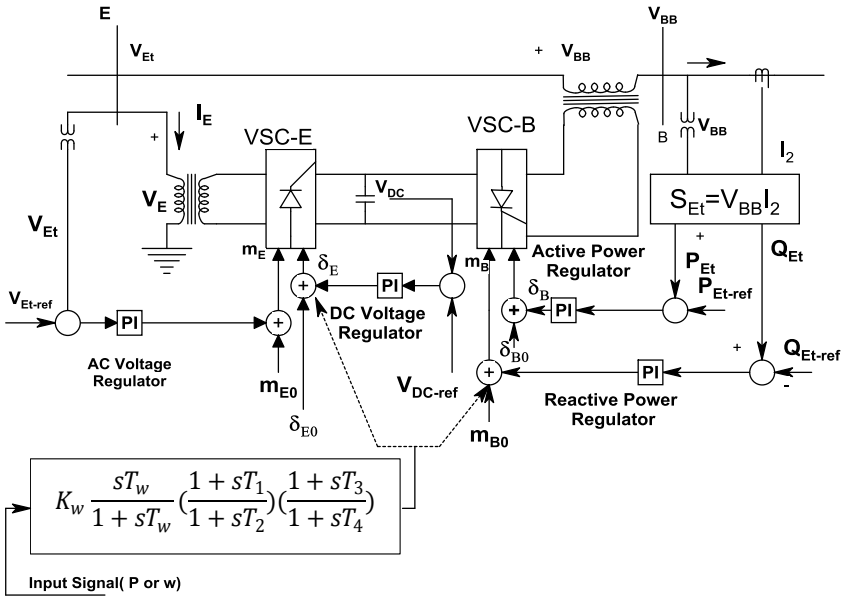

Fig. 1. UPFC power and control flow diagram

A supplementary controller, known as POD, is designed in UPFC to enhance transient stability of the entire electric power system. Inverse interaction between PSS and series part control is compensated by providing a UPFC-based damping controller [19]. As shown in figure 1, POD controller have a lead-lag controller structure transfer function consisting of a gain, a washout function and two lead-lag blocks, which should be adjusted. Fixed parameter classical

controller is not suitable for the UPFC damping control design. Then, a flexible controller should be developed. Several approaches have been propose for it, such as root locus and sensitivity analysis, pole placement, and robust control. The conventional techniques require heavy computation and have slow convergence. Search methods may also trap in a local minimum and obtained solution may not be the finest. In addition, it is necessary that the designed controller provide some robustness to the variations of parameters, conditions, and configurations. Also, the controller parameters which stabilize the system in a certain operating condition may no longer have acceptable results in case of large disturbances [20].

To improve its dynamic performance, its parameters can optimize by forming an optimization problem with defining an objective function based on eigenvalues and damping ratio expressed in (6):

$$J = \sum_{j=1}^{NP} \sum_{\sigma_i \geq \sigma_0} (\sigma_0 - \sigma_{ij})^2 + \alpha \sum_{j=1}^{NP} \sum_{\zeta_i \geq \zeta_0} (\zeta_0 - \zeta_{ij})^2 f(x) \quad (6)$$
$$= \min J$$

$$K^{\min} \leq K \leq K^{\max}$$
$$T_1^{\min} \leq T_1 \leq T_1^{\max}$$
$$T_2^{\min} \leq T_2 \leq T_2^{\max}$$
$$T_3^{\min} \leq T_3 \leq T_3^{\max}$$
$$T_4^{\min} \leq T_4 \leq T_4^{\max}$$

Where σ_{ij} are real parts of system Eigen values and σ_0 is desired real part of Eigen value, ζ_{ij} are damping ratios of system variables and ζ_0 is desired damping ratio. This optimization problem can solve by a numerical techniques such as PSO

3. Introduction to DFIG study

In DFIG, two converters are included in the rotor circuit. The power electronic converters ratio is a fraction of the total power. Therefore, the losses in the power electronic converter can be reduced, compared to a system where the converter has to handle the entire power, and the system cost is lower due to the partially rated power electronics. DFIG operates in both sub-synchronous and super-synchronous modes with a rotor speed range around the synchronous speed. Then, in variable-speed systems DFIG offers adequate performance [21]. Figure 2 shows the a DFIG-based wind farm connected to a power system.

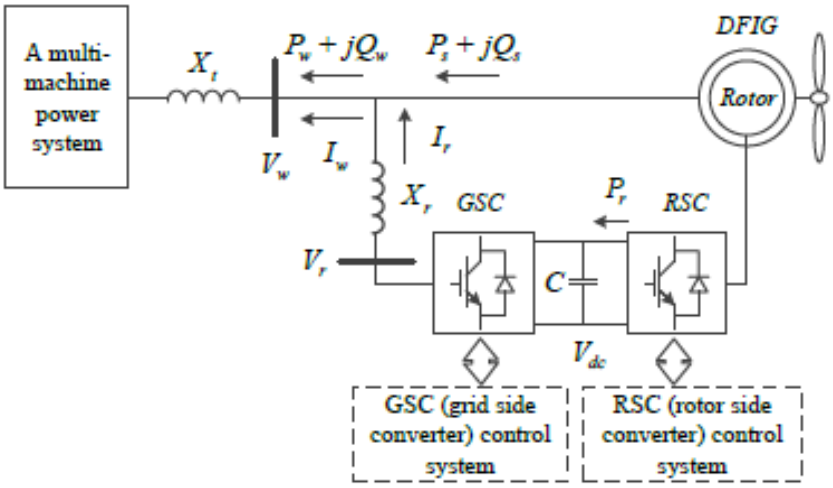

Fig. 2. DFIG schematic connection to multi-machine power system

In [22] different state space models of DFIG for power system study have been compared. The modeling detail of the turbine, drive train ,pitch controller, induction machine and the controllers of both rotor-side converter (RSC) and the grid-side converter (GSC) of DFIG have introduced.

DFIG state equations in dynamic stability studies have described in the following:

Equations (7)-(10) express two-mass model of turbine drive dynamic, and (11)-(13) are three-degree model of induction machine.

$$2H_t \frac{d\omega_t}{dt} = T_m - T_{sh} \quad (7)$$

$$2H_g \frac{d\omega_g}{dt} = T_{sh} - T_e \quad (8)$$

$$\frac{1}{\omega_b}\frac{d\theta_{tw}}{dt} = \omega_t - \omega_g \quad (9)$$

$$T_{sh} = D\frac{d\theta_{tw}}{dt} + K\theta_{tw} \quad (10)$$

$$T_0'\frac{dE_{qD}'}{dt} = -\left(E_{qD}' + (X_s - X_s')I_{ds}\right) + T_0'\left(\omega_s\frac{X_m}{X_r}V_{dr} - (\omega_s - \omega_r)E_{dD}'\right) \quad (11)$$

$$T_0'\frac{dE_{dD}'}{dt} = -\left(E_{dD}' + (X_s - X_s')I_{qs}\right) + T_0'\left(\omega_s\frac{X_m}{X_r}V_{qr} - (\omega_s - \omega_r)E_{qD}'\right) \quad (12)$$

$$2\frac{H_D}{\omega_s}\frac{d\omega_r}{dt} = T_m - E_{dD}'I_{ds} - E_{qD}'I_{qs} \quad (13)$$

Where:

$$V_{qs} = -R_sI_{qs} - X_s'I_{ds} + E_{qD}'$$
$$V_{ds} = -R_sI_{ds} + X_s'I_{qs} + E_{dD}'$$
$$I_{dr} = \frac{E_{qD}'}{X_m} + \frac{X_m}{X_r}I_{ds}\ ,\quad I_{qr} = -\frac{E_{dD}'}{X_m} + \frac{X_m}{X_r}I_{qs}$$
$$T_0' = \frac{X_r}{\omega_sR_r}\ ,\ X_s' = X_s - \frac{X_m^2}{X_r}$$
$$E_{qD}' = \frac{X_m}{X_r}\varphi_{qr}\ ,\quad E_{dD}' = -\frac{X_m}{X_r}\varphi_{qr}$$

Equations (14)-(17) for grid side converter PI controllers and equations (18)-(21) for rotor side converter PI controller are as follow:

$$\Delta x_1 = \frac{1}{K_{I1}}\left(V_{dc\,Ref} - V_{dc}\right) \quad (14)$$

$$\Delta x_2 = \frac{1}{K_{I2}}\left(i_{qg} - \left(-x_1 + K_{P1}\left(V_{dc\,Ref} - V_{dc}\right)\right)\right) \quad (15)$$

$$\Delta x_3 = -\frac{1}{K_{I3}}\left(V_{s\,Ref} - V_s\right) \quad (16)$$

$$\Delta x_4 = \frac{1}{K_{I4}}\left(i_{dg} - \left(x_3 - K_{P3}\left(V_{s\,Ref} - V_s\right)\right)\right) \quad (17)$$

$$\Delta x_5 = \frac{1}{K_{I5}}\left(\omega_{Ref} - \omega_r\right) \quad (18)$$

$$\Delta x_6 = \frac{1}{K_{I6}}\left(i_{qr} - \left(x_5 + K_{P5}\left(\omega_{Ref} - \omega_r\right)\right)\right) \quad (19)$$

$$\Delta x_7 = \frac{1}{K_{I7}}\left(Q_{s\,Ref} - Q_s\right) \quad (20)$$

$$\Delta x_8 = \frac{1}{K_{I8}}\left(i_{dr} - \left(x_7 + K_{P7}\left(Q_{s\,Ref} - Q_s\right)\right)\right) \quad (21)$$

Where, above variables are according to figure 2. V_s is stator voltage. i_g and i_r and ω_r are grid and rotor side converters ac currents and rotor angular speed respectively. auxiliary variables x_1 to x_8 which have defined to consider rotor and grid side converters dynamic. Equation (22) represents DC link capacitor between two converters dynamic:

$$C_DV_{DC}\frac{dV_{DC}}{dt} = \left(v_{dr}i_{dr} + v_{qr}i_{qr}\right) - \left(v_{dg}i_{dg} + v_{qg}i_{qg}\right) \quad (22)$$

4. Modeling of power system with UPFC installed

The performance analysis of UPFC require its steady-state and dynamic models. Figure 3 shows UPFC in multi-machine power system:

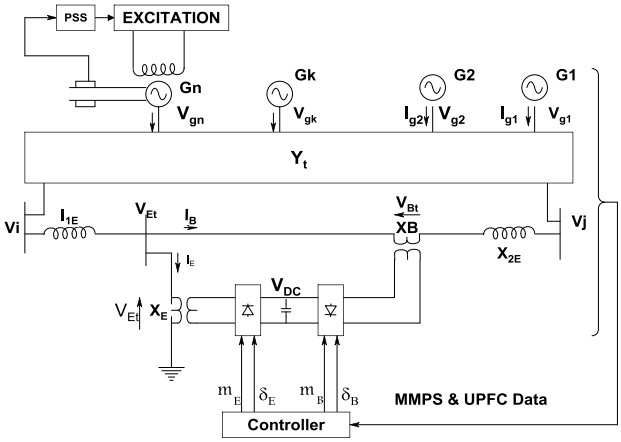

Fig. 3. UPFC incorporated in the multi-machine power system

With reducing the bus admittance matrices to generator internal buses and UPFC terminal buses the following equation can be written:

$$\bar{Y}\bar{E} = \bar{I}\ ,\quad \bar{Y} = \begin{bmatrix} Y_{GG} & Y_{GU} \\ Y_{UG} & Y_{UU} \end{bmatrix},\ \bar{E} = \begin{bmatrix} \bar{E}_G \\ \bar{V}_U \end{bmatrix},\ \bar{I} = \begin{bmatrix} \bar{I}_G \\ \bar{I}_U \end{bmatrix} \quad (23)$$

Where:

$Y_{GG}$is the reduced admittance matrices connecting the generator current injection to the internal generator voltages. Y_{GU} is the admittance matrices component which gives the generator currents due to the voltages at UPFC buses. Y_{UG} is the admittance matrices component which gives UPFC currents in terms of the generator internal voltages. Y_{UU} is the admittance matrices connecting UPFC currents to the voltages at UPFC buses. $\bar{E}_G$ is the vector of generator internal

bus voltages. $\overline{V}_U$ is vector of UPFC ac bus voltages. $\overline{I}_G$ is the vector of generator current injections. $\overline{I}_U$ is the vector of UPFC currents injected to the power network. Then these parameters values will incorporate in deriving matrices equation of multi machine power system with UPFC installed which is essential in dynamic stability analysis.

For the small signal stability studies of the power system, the linear model of Heffron-Phillips is used which provides reliable and enough accurate results [23]. The nonlinear dynamic model of the system installed with the UPFC equations are as follows:

$$\dot{\delta} = \omega_b(\omega - 1) \tag{24}$$

$$\dot{\omega} = M^{-1}(T_m - T_e - D(\omega - 1) \tag{25}$$

$$\dot{E}'_q = T'_{do}(E_{fd} - E'_q + (X_d - X'_d)I_d) \tag{26}$$

$$\dot{E}_{fd} = (K_A(V_{Ref} - V_t) - E_{fd})/T_A \tag{27}$$

$$\dot{V}_{DC} = \frac{3m_E}{4C_{dc}}(sin\delta_E I_{Ed} + cos\delta_E I_{Eq}) + \frac{3m_B}{4C_{dc}}(sin\delta_B I_{Bd} + cos\delta_B I_{Bq}) \tag{28}$$

These equations can be rewritten and after linearization in the following matrices form. Detail value calculation of K coefficients introducedd in [16]:

$$\begin{bmatrix} \Delta\dot{\delta} \\ \Delta\dot{\omega} \\ \Delta\dot{E}'_q \\ \Delta\dot{E}_{fd} \\ \Delta\dot{V}_{DC} \end{bmatrix} = \begin{bmatrix} 0 & \omega_0 I & 0 & 0 & 0 \\ -M^{-1}K_1 & -M^{-1}D & -M^{-1}K_2 & 0 & -M^{-1}K_{pd} \\ -T_{do}^{-1}K_4 & 0 & -T_{do}^{-1}K_3 & T_{do}^{-1} & -T_{do}^{-1}K_{qd} \\ -T_A^{-1}K_5K_A & 0 & -T_A^{-1}K_6K_A & -T_A^{-1} & -T_A^{-1}K_6K_{vd} \\ K_7 & 0 & K_8 & 0 & -K_9 \end{bmatrix} \begin{bmatrix} \Delta\delta \\ \Delta\omega \\ \Delta E'_q \\ \Delta E_{fd} \\ \Delta V_{DC} \end{bmatrix} + \begin{bmatrix} \mathbf{0} & \mathbf{0} & \mathbf{0} & \mathbf{0} \\ -\mathbf{M^{-1}K_{pe}} & -\mathbf{M^{-1}K_{pde}} & -\mathbf{M^{-1}K_{pb}} & -\mathbf{M^{-1}K_{pdb}} \\ -\mathbf{T_{do}^{-1}K_{qe}} & -\mathbf{T_{do}^{-1}K_{qde}} & -\mathbf{T_{do}^{-1}K_{qb}} & -\mathbf{T_{do}^{-1}K_{qdb}} \\ -\mathbf{T_A^{-1}K_AK_5} & -\mathbf{T_A^{-1}K_AK_{vde}} & -\mathbf{T_A^{-1}K_AK_{vb}} & -\mathbf{T_A^{-1}K_AK_{vdb}} \\ K_{ce} & K_{cde} & K_{cb} & K_{cdb} \end{bmatrix} \begin{bmatrix} \Delta m_E \\ \Delta\delta_E \\ \Delta m_B \\ \Delta\delta_B \end{bmatrix} \tag{29}$$

As we can see above equation is the standard form of the linear system as below:

$$\Delta\dot{X}_g = A_g\Delta X_g + B_g\Delta U \tag{30}$$

This matrices equation is suitable for classical linear control and numerical solving the system equations as well as analysis such as Eigen values related techniques.

5. Modeling of DFIG connected to power system

Recently researchers have shown that in a modal study if wind farm is replaced by an equal dynamic DFIG it will have acceptable result [24]. A comprehensive model of DFIG, connected to a power system, similar to Wang' [17] idea which has done before for FACTS devices has developed [25]. Multi-machine power system linearized model considering in which a DFIG connected such as figure 2 may be extract as follow:

$$\frac{d}{dt}\begin{bmatrix} \Delta\delta \\ \Delta\omega \\ \Delta E'_q \\ \Delta E_{fd} \end{bmatrix} = \begin{bmatrix} 0 & \omega_0 I & 0 & 0 \\ -M^{-1}K_1 & -M^{-1}D & -M^{-1}K_2 & 0 \\ -T_{do}^{-1}K_4 & 0 & -T_{do}^{-1}K_3 & T_{do}^{-1} \\ -T_A^{-1}K_5K_A & 0 & -T_A^{-1}K_6K_A & -T_A^{-1} \end{bmatrix} \begin{bmatrix} \Delta\delta \\ \Delta\omega \\ \Delta E'_q \\ \Delta E_{fd} \end{bmatrix} + \begin{bmatrix} 0 \\ -M^{-1}k_{PP} \\ -T_{do}^{-1}k_{EP} \\ T_A^{-1}K_Ak_{VP} \end{bmatrix}\Delta P_W + \begin{bmatrix} 0 \\ -M^{-1}k_{PQ} \\ -T_{do}^{-1}k_{EQ} \\ T_A^{-1}K_Ak_{VQ} \end{bmatrix}\Delta Q_W \tag{31}$$

The state vector of the whole grid, X_g, in the matrix format while DFIG is as follows:

$$\frac{d}{dt}\Delta X_g = A_g\Delta X_g + b_P\Delta P_w + b_Q\Delta Q_w \tag{32}$$

V_W is the bus by which DFIG connected to power system voltage amplitude that can be represented as below:

$$\Delta V_W = C_g\Delta X_g + d_{g1}\Delta P_W + d_{g2}\Delta Q_W \tag{33}$$

DFIG linearized model can be used in the following format:

$$\frac{d}{dt}\Delta\Psi_{wsd} = K_{wd1}\Delta\Psi_{wsd} + K_{wq1}\Delta\Psi_{wsq} + \cdots + K_{1V}V_w \tag{34}$$

$$\frac{d}{dt}\Delta\Psi_{wsq} = K_{wd2}\Delta\Psi_{wsd} + K_{wq2}\Delta\Psi_{wsq} + \cdots + K_{2V}V_w \tag{35}$$

For any other selected state variable of DFIG:

$$\frac{d}{dt}\Delta x_j = K_{wdj}\Delta\Psi_{wsd} + K_{wqj}\Delta\Psi_{wsq} + \cdots + K_{jV}V_w \tag{36}$$

In matrix format:

$$\frac{d}{dt}\Delta X_w = A_w(p)\Delta X_w + b_w(p)\Delta V_W \tag{37}$$

Output power of DFIG in linear form can be shown as:

$$\begin{bmatrix} \Delta P_w \\ \Delta Q_w \end{bmatrix} = \begin{bmatrix} c_{Pw}^T \\ c_{Qw}^T \end{bmatrix}\Delta X_w + \begin{bmatrix} c_{PV} \\ c_{QV} \end{bmatrix}\Delta V_w \tag{38}$$

We can replace them in Heffron-philips equations to form matrix format equations containing both

power system and DFIG variables:
Here we have used a more complete model of DFIG so that the state variable vector of DFIG is:

$$\Delta X_w = [\Delta\Psi_{wsd}\ \Delta\Psi_{wsq}\ \Delta\Psi_{wrd}\ \Delta\Psi_{wrq}\ \Delta\omega_{r1}\ \Delta\omega_{r2}\ \Delta\theta_{wr}\ \Delta x_{w1}\ \Delta x_{w2}\ \Delta x_{w3}\ \Delta x_{w4}\ \Delta I_{dcd}\ \Delta I_{dcq}\ \Delta V_{wdc}\Delta x_{w5}\ \Delta x_{w6}\ \Delta x_{w7}]^T \quad (39)$$

Where w index refers to wind (DFIG) parameters, s represents the stator, r represents the rotor, d represents the d axis, q represents the q axis and dc represents the dc link. To consider RSC and GSC dynamic, $\Delta x_{w1}$to Δx_{w7} as linearized auxiliary variables have defined.

Combining (32),(33) and (38) will form dynamic equation for both systems as follow:

$$\begin{bmatrix}\Delta\dot{X}_g\\ \Delta\dot{X}_w\\ \Delta\dot{X}_c\end{bmatrix} = A\begin{bmatrix}\Delta X_g\\ \Delta X_w\\ \Delta X_c\end{bmatrix} \quad (40)$$

X_c is the state variables related to PI controllers of DFIG control system.

To dynamic stability study of the whole system, we should combine (30) and (40) to reach to (41) which explain multi-machine power system simultaneously contains UPFC and DFIG and we can use it to investigate small signal issues of whole system.

$$\Delta\dot{X} = A\Delta X + B\Delta U \quad (41)$$

While:

$$\Delta X = \begin{bmatrix}\Delta X_g\\ \Delta X_W\\ \Delta X_c\\ \Delta V_{DC}\end{bmatrix} \quad (42)$$

Dimension of this state vector is *4n+1+17*. n is the number of synchronous generators, 1 state for UPFC and 17 state for DFIG while 7 of them are auxiliary to express PI controllers. We use (41) to design control system and if need we can do any compromising, co-ordination, optimization using this last overall matrix linear equation.

6. Particle swarm optimization algorithm

PSO is an optimization technique which is population-based to solve the optimization problem with constraint. In PSO system, multiple solutions are candidate and collaborate simultaneously. Each candidate, called a particle, flies in the problem search space looking to land on the optimal position. particles, during the generations, adjusts their own positions according to their's own experience and the experience of neighbor particles. This algorithm tries to balance exploitation and exploration by combine global and local search methods, and. New velocity and position of each particle will be updated according to the following equations [15]:

$$V_i[k+1] = wV_i[k] + c_1r_1(pbest_i[k] - X_i[k]) + c_2r_2(gbest[k] - X_i[k])\ ,i = 1,2,\ldots, \quad (44)$$

$$X_i[k+1] = X_i[k] + V_i[k+1] \quad (45)$$

Where N is the number of particles, k is the current iteration, w is an inertia weight, r_1 and r_2 are random variables between 0 and 1, c_1 and c_2 are acceleration coefficients. V_i and X_i are the velocity and position of the particle i respectively. $pbest_i$ is the local best position of particle i. $gbest$ is the global- best position of all particles.

Both Genetic Algorithm and PSO have used to optimize a.m. functions in this study. Here PSO results have used due to new progress in PSO and its faster response in compare with GA. The PSO have used three times; (a) to optimize J function that mentioned above with PSO the lead-lag controller parameters; T_1 to T_4 and wash-out gain K are adjusted while only UPFC have used in power system. (b); To optimize similar J function (based on Eigen values) to optimize the values of 7 PIs of RSC and GSC of DFIG while only DFIG connected to power system. (c) To optimize the same function for the whole system to optimize UPFC POD parameters and DFIG PIs parameters simultaneously.

7. System simulation

7.1. Implementation algorithm

We applied this simulation method to several power systems and we report the results of one of them here. Figure 4 shows the studied power system which is a 10-machine 39-bus New England network whose data can be found in [26]. For small signal analysis the sampling time was selected as 0.1 m.sec. thus the frequency of the two UPFC and DFIG inverters parameters updating is 10khz which is consistent with the existing switches speeds. In this study PSS was

used only for the generator that is installed on the slack bus, because PSS was not our study subject, and to prevent its interaction with other controllers and system modes. It contains wash out and two lead lag blocks and its parameters have tuned using PSO with ITAE criteria objective function before UPFC and DFIG insertion.

To three phase earth fault case study, it is simulated four scenarios; power system without UPFC and without DFIG, power system using UPFC controller only, power system while DFIG (wind farm) is connected, power system while both UPFC and DFIG controllers are simultaneously designed and used to have better dynamic stability.

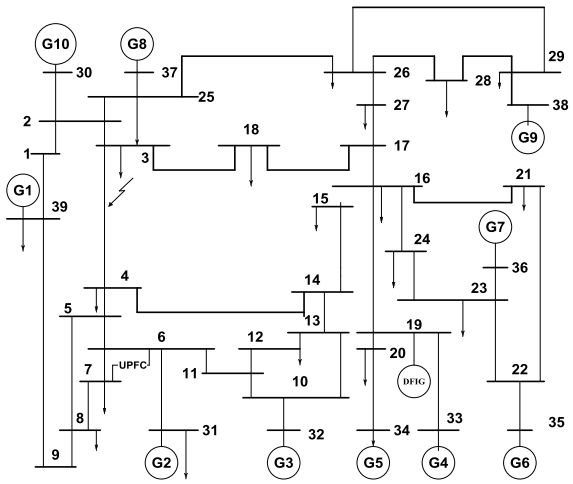

Fig. 4. New England power system network schematic single line diagram

7.2. Power system simulation results

In this study, MATLAB program was used to simulate the model. Within the load flow solution the thermal limits of lines capacity are considered. Three phase earth fault is applied to the line between bus 3 and 4 and its duration to clear is 0.1 sec which is short enough for small signal analysis. Oscillations are demonstrated by extracting $\Delta\delta$ and $\Delta\omega$ of all machines. Figure 5 depicts the results while DFIG is not connected and UPFC is not installed. The results of load flow implementation are used to find UPFC placement to improve voltage profile.

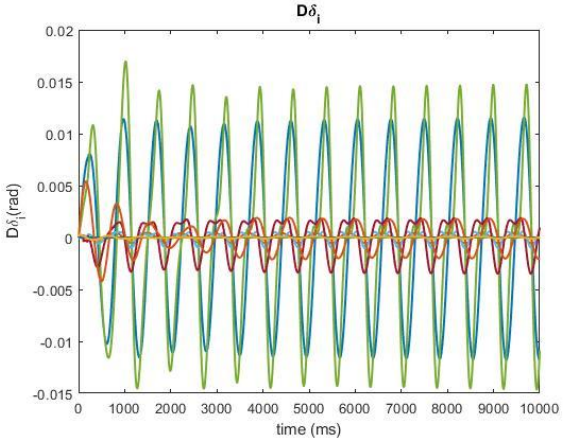

(a) All machines load angle deviations in power system without both UPFC and DFIG

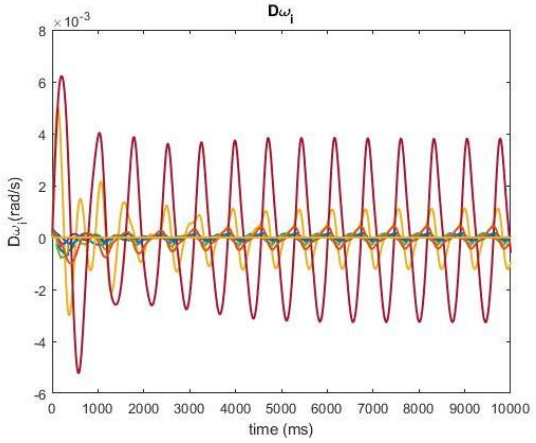

(b) All machines speed deviations in power system without both UPFC and DFIG

Fig 5. All machines oscillations in power system without both UPFC and DFIG

7.3. Power system using UPFC controller

Result of load flow implementation is used to find UPFC placement to improve voltage profile and load flow of power system. Within the load flow solution the thermal limits of lines capacity are considered. After the UPFC insertion in the power network the load flow is executed again. Minimizing total power loss of power system and acceptable voltage profile were two criteria to UPFC placement. UPFC is installed between 6 and 7 buses in the system, the active and reactive power losses are reduced. It is also verified that not only the power losses are reduced, the voltage profile of the buses is improved after incorporating UPFC too. This simulation is carried out according to flowchart in figure 6.

For small signal and dynamic stability study we used UPFC dynamic model and interfacing

with power system as described in section 4. All four basic controllers of UPFC are considered. Eigenvalues and damping ratios of the linearized system are derived and based on these values the PSO algorithm is used to optimize damping oscillations controller. Figure 7 demonstrate the eigenvalues of the system with and without UPFC in complex plane. As we can see some of eigenvalues have a little more negative real part.

To investigate the enhancement of the power system stability by a UPFC, we studied the results and responses of three phase earth fault scenarios too. Figure 8(a) shows four UPFC parameters and 8(b) faulted bus voltage and 8(c) the variation of all machines load angle variations 8(d) all machines speed variations with three phase earth fault applied.

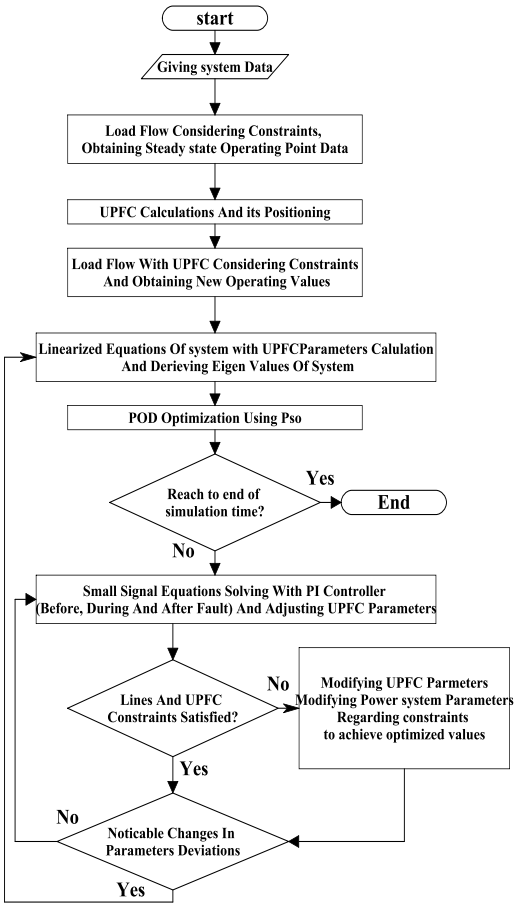

Fig. 6. The Flowchart of the simulation of the power system with the UPFC installed

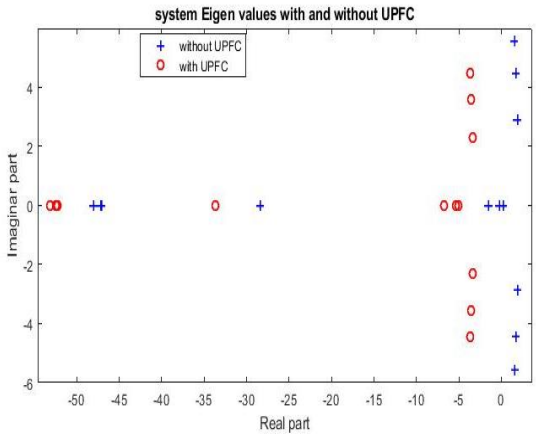

Fig. 7. Comparison of System Eigen values with and without UPFC

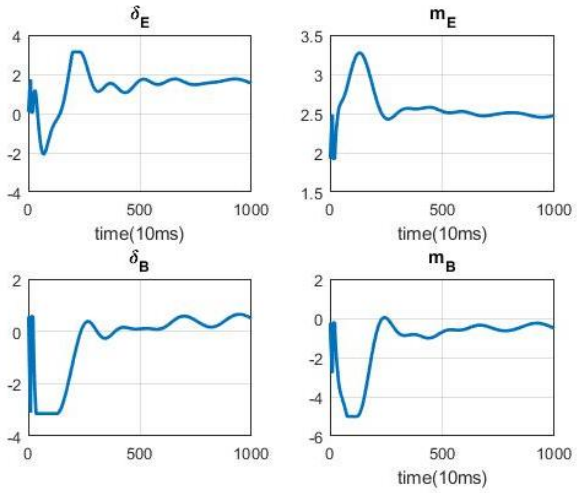

(a)UPFC four parameters in the power system three phase earth fault

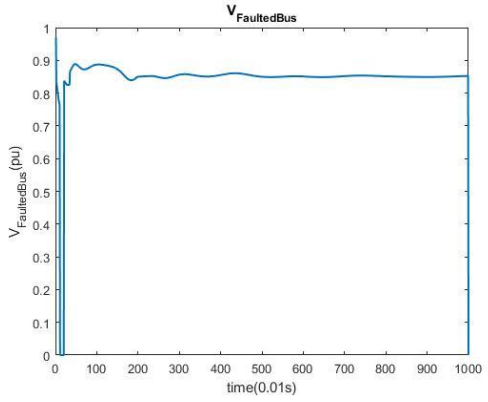

(b) Faulted bus voltage in the power system three phase earth fault while only UPFC installed

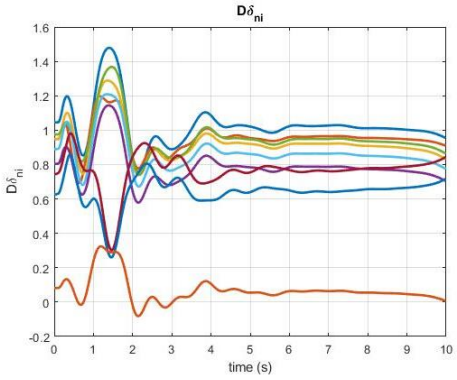

(c) All machines load angle deviations in the power system three phase earth fault while only UPFC installed

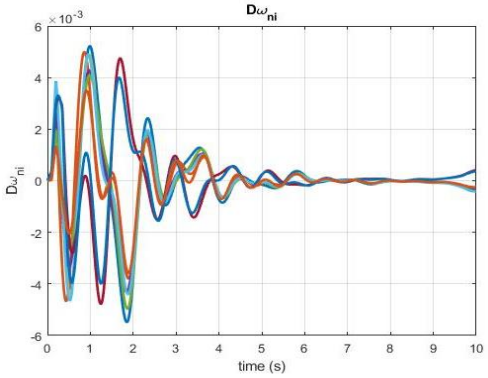

(d) All machines speed deviations in power system three phase earth fault while only UPFC installed

Fig. 8. Damping performance and effect of UPFC in three phase earth fault

7.4. Power system using connected DFIG

DFIG place which depends on weather and geographical conditions according to [27] has selected. While DFIG (connected to bus 19 with a short line) controller is used to damp oscillation we can see that it's effect is less than when we used UPFC. But we found that while we increased the capacity of wind farm (equal DFIG), it's effect on oscillation damping will increased too. This simulation is carried out according to flowchart in figure 9. Figure 10(a) shows the variation of all machines load angle variations, 10(b) all machines speed variations and figure 10(c) the DFIG states which expressed in (39).

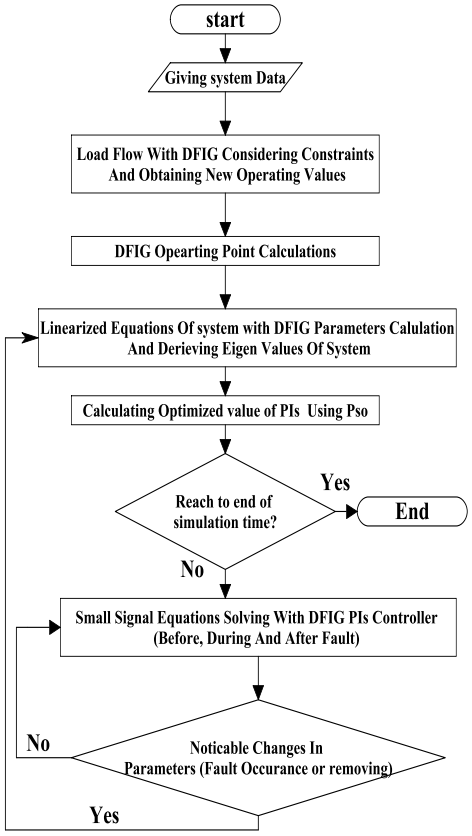

Fig. 9. The Flowchart of the simulation of the power system with the DFIG connected

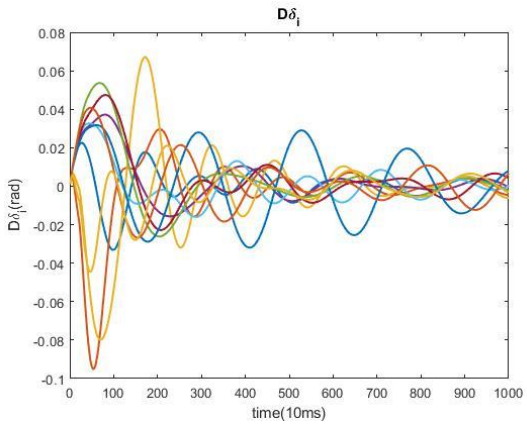

(a) All machines load angle deviations while only the DFIG have connected

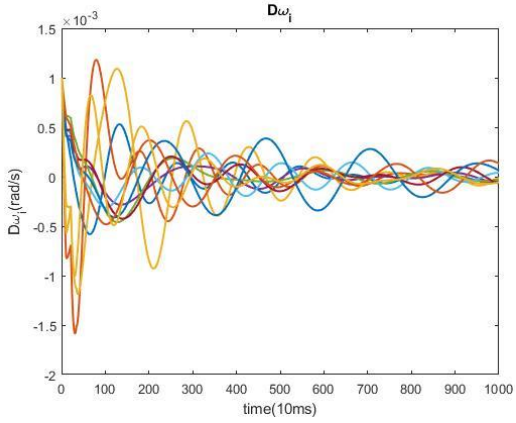

(b) All machines speed deviations while only the DFIG have connected

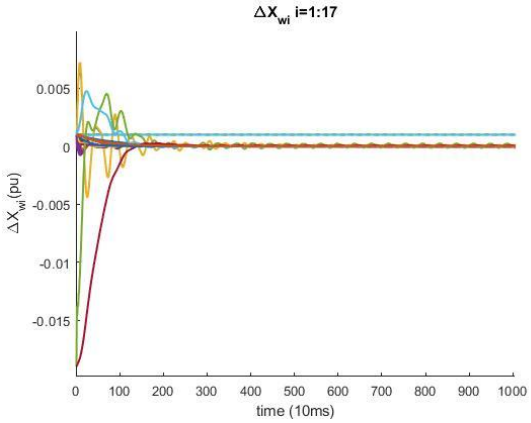

(c) DFIG states deviations while only the DFIG have connected

Fig. 10. Damping effect of DFIG in three phase earth fault

7.5. Power system using both UPFC and DFIG controller

According to flowchart in figure 11, the whole system linearized equation which showed in (41) is used to optimize parameters of both UPFC and DFIG and solve to extract variables deviation. While there are both UPFC and DFIG in power system controllers, they are adjusted in one state matrix simultaneously and are coordinated. Results show that the damping effect of them is better than when we use their controller with individual design of them. Figure 12(a) shows all machines load angle variations, 12(b) all machines speed variations and figure 12(c) the DFIG states which expressed in equation (39) respectively.

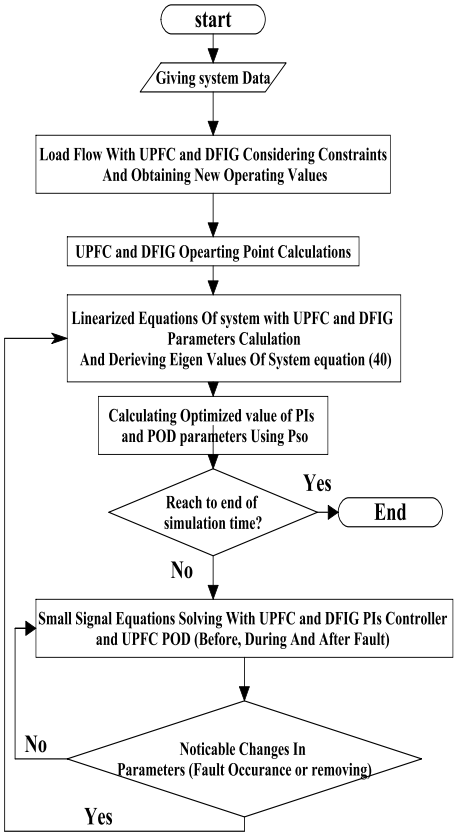

Fig. 11. The Flowchart of the simulation of the power system with the DFIG connected and the UPFC installed

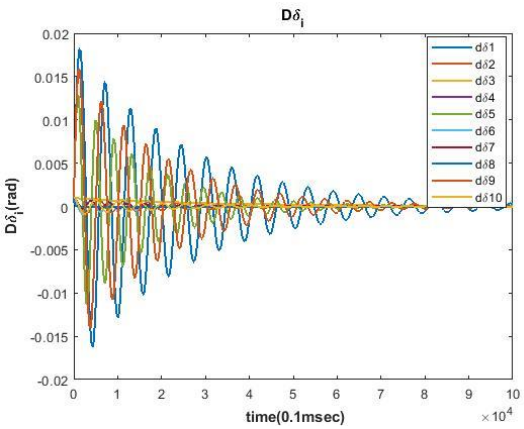

(a) All machines load angle deviations while the power system consisting both UPFC and DFIG

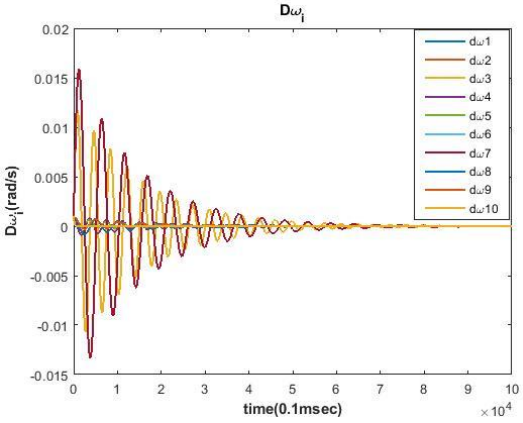

(b) All machines speed deviations while the power system consisting both UPFC and DFIG

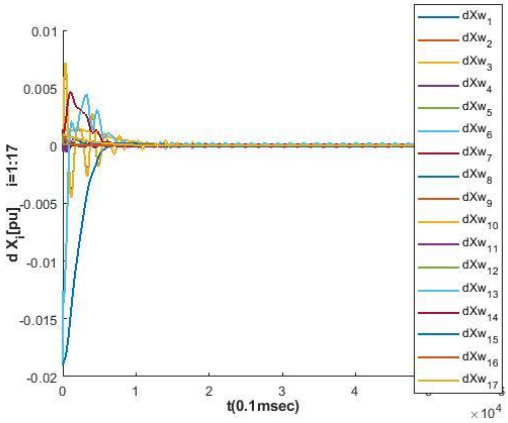

(c) DFIG states deviations while the power system consisting both UPFC and DFIG

Fig. 12. Damping effect of both UPFC and DFIG in earth fault while coordinated designed

7.6. Line outage scenario study

In same power system, it is assumed that the same line (line connected from bus 3 to bus 4) outage has occurred. Same three different cases i.e. (i) system with only UPFC installed, (ii) system with only DFIG connected and (iii) system containing both DFIG and UPFC have studied too. The results of simulations demonstrated in Fig. 13. Figure 13(a) and 13(b) show all machines load angle deviations and speed deviations respectively while the power system equipped only with UPFC. Figure 13(c) and 13(d) show all machines load angle deviations and speed deviations respectively while the power system containing only DFIG. Figure 13(e) and 13(f) show all machines load angle deviations and speed deviations respectively while the power system consisting both UPFC and DFIG.

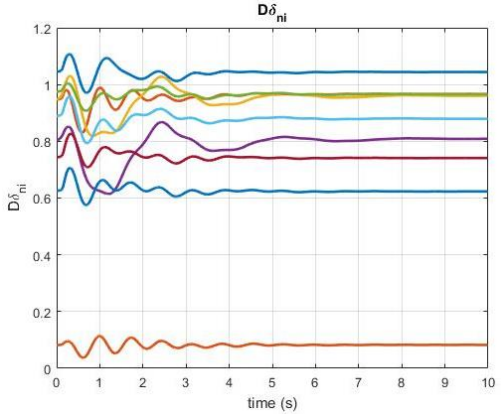

(a) All machines load angle deviations in the power system line outage while only UPFC installed

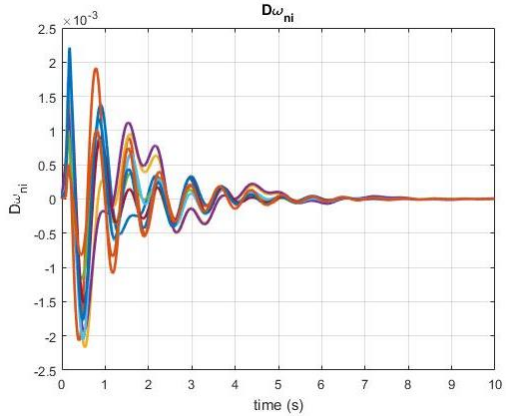

(b) All machines speed deviations in the power system line outage while only UPFC installed

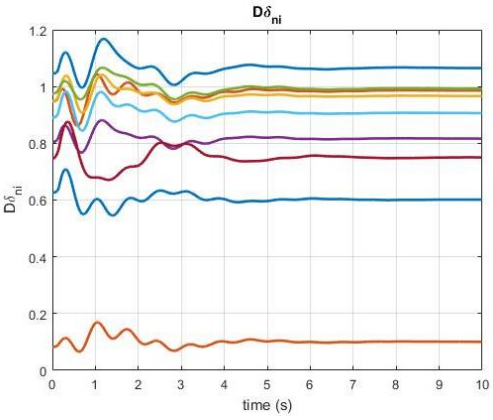

(c) All machines load angle deviations in the power system line outage while only DFIG connected

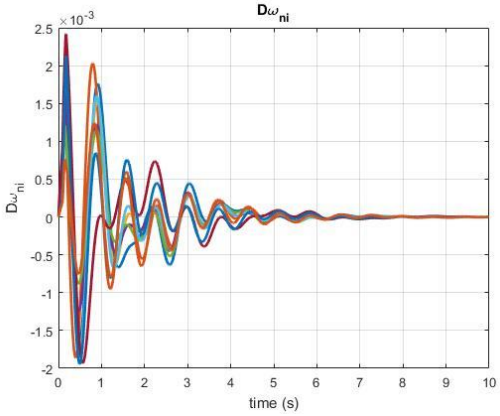

(d) All machines speed deviations in the power system line outage while only DFIG connected

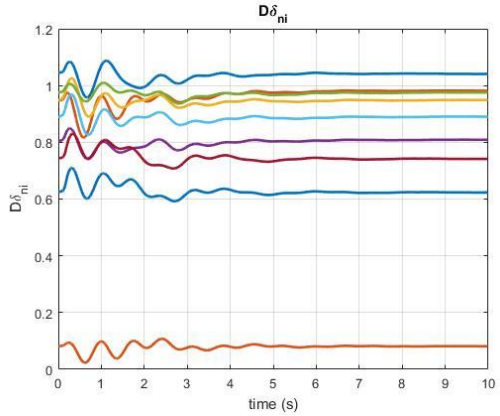

(e) All machines load angle deviations in the power system line outage while both UPFC and DFIG have used

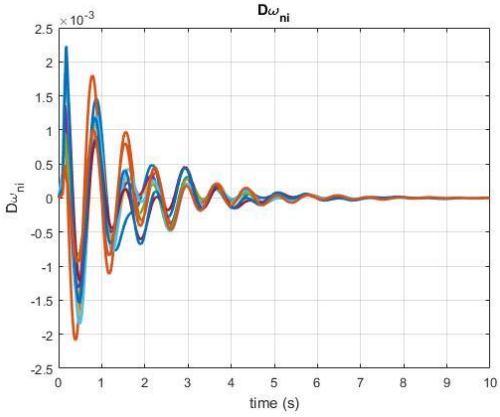

(f) All machines speed deviations in the power system line outage while both UPFC and DFIG have used

Fig. 13. Line outage scenario three cases results

8. Conclusions

In this study, power system with UPFC and its all four main controllers and its damping controller modeled to incorporate in the 10-machine 39-bus new England multi-machine power system Heffron-Philips model. DFIG small signal modeling carried out considering its 17 state variables. At first the individual effect of the UPFC and the DFIG on dynamic stability have studied. Then their linearized model incorporated in the same power system model together. Finally modal analysis and dynamic stability of the whole system have studied.

Response and behavior of several main modes of the power system after three phase earth fault and line outage investigated. The results show that the UPFC can noticeably improve dynamic stability of the whole power system. And control of the DFIG in the power system helps the control system to improve dynamic stability of the DFIG and the power system. When there are both of these two devices in the multi-machine power system, coordinating and making optimization in both the UPFC parameters and controllers and the DFIG controllers simultaneously, results improvement in the dynamic stability of the multi machine power system. As it is obvious, almost all of machines and DFIG state variables oscillations have noticeable faster damping and less overshoots and settling times in three phase earth fault and line outage scenarios as two main power system contingencies.

Appendixess

The UPFC data:

In 39-bus New England network:

UPFC Rating=190 MW=1.9 pu, xE= 0.0725 pu, xB=0.0725 pu, C=1 pu, Sb=100MW.

The DFIG data:

Mw=3.4, Dwm=0, Rwr=0.0007, Kwm=3.95, Jwr1=8, Jwr2=8, Dwr1=0.0, wr2=0.0, Xws=0.0878, Xwr=0.0373, Xwm=1.3246, Xwr3=0.05, Xwf=0.05, sw0=-0.01, Cw=13.29, Rws=0, DFIG rating power=56MW=0.56 pu

References

[1] A. Ziaei , R. Ghazi , R. Zeinali davarani, “Linear Modal Analysis of Doubly-Fed Induction Generator (DFIG) Torsional Interaction: Effect of DFIG Controllers and System Parameters", Advances in Electrical and Electronic Engineering, pp. 388-401, 2018.

[2] M. Ravindrababu, G. Saraswathi, K.R. Sudha, “Design of UPFC-PSS using Firefly Algorithm for Stability Improvement of Multi Machine System under Contingency”, Majlesi Journal of Electrical Engineering , Vol. 13, No. 2, pp. 21-39, June 2019.

[3] B. K. Dubey, N.K. Singh, “Multimachine Power System Stability Enhancement with UPFC Using Linear QUADRATIC Regulator Techniques”, International Journal of Advanced Research in Engineering and Technology (IJARET), Vol. 11, Issue 4, pp. 219-229, April 2020.

[4] N. Nahak, R. K. Mallick, S. P. Muni, "Stability Enhancement of Multi machine System by Improved GWO Optimized UPFC based controller", International Journal of Pure and Applied Mathematics, Vol. 114, No. 9, pp. 63-72, 2017.

[5] S.Q. Bu, X. Zhang, J.B. Zhu, X. Liu, "Comparison analysis on damping mechanisms of power systems with induction generator based wind power generation", Electrical Power and Energy Systems, pp. 250–261, 2018.

[6] Y. Mohammed, R. Alharbi, "Application of Unified Power Flow Controller to Improve the Performance of Wind Energy Conversion System", Phd thesis, Department of Electrical and Computer Engineering, Curtin University, March 2016.

[7] S. Biswas, "Application of Unified Power Flow Controller in DFIG Based Wind Turbine", International Journal of Science and Research (IJSR), Vol. 3 Issue 6, pp. 744-748, June 2014.

[8] P. Khandelwal, B. Modi, S. S. Sharma, "DFIG based WECS Connected Power System Using UPFC for Improvement of Stability", Vol. I, Issue IV, pp. 10-15, September 2014.

[9] A. Ganesan, R. Rajamoort, "Modeling of FUZZY Controlled UPFC for LVRT Improvement in DFIG Based Grid Connected Wind Farm", Journal of Electronic Design Engineering, Vol. 5 Issue 1, pp. 29-38, MAT Journals 2019.

[10] M. Ferdosian, H. Abdi, A. Bazaei , "Improving the Wind Energy Conversion System Dynamics during Fault Ride through: UPFC versus STATCOM", IEEE 2015 IEEE International Conference on Industrial Technology (ICIT), pp. 2721-2726, 2015.

[11] Y. M. Alharbi, A. M. S.Yunus, A. Abu-Siada, "Application of UPFC to Improve the FRT Capability of Wind Turbine Generator", International Journal of Electrical Energy, Vol. 1, No. 4, pp. 188-193, December 2013.

[12] Nidhi Vaishnava Amit Verma , Performance Analysis of DFIG based Wind Turbine System using FACTS Devices , International Journal of Science Technology & Engineering, | Vol. 4, Issue 1, pp. 178-183, July 2017.

[13] P. K. Dash, R. K. Patnaik, S. P. Mishra, Adaptive fractional integral terminal sliding mode power control of UPFC in DFIG wind farm penetrated multimachine power system, Protection and Control of Modern Power Systems (2018) 3:8, pp. 1-14, 2018.
https://doi.org/10.1186/s41601-018-0079-z.

[14] D. E. Tourqui, M. Benakcha, T. Allaoui, "Improving the Electrical Stability by Wind Turbine and UPFC, Improving the Electrical Stability by Wind Turbine and UPFC", Artificial Intelligence in Renewable Energetic Systems, Springer International Publishing AG 2018. https://doi.org/10.1007/978-3-319-73192-6_13.

[15] Y. Shi, R. Eberhart, "A modified particle swarm optimizer", IEEE international conference on evolutionary computation proceedings, Anchorage, AK, USA, pp. 69–73, 1998.

[16] A. Nabavi-Niaki, M.R. Iravani, "Steady-state and dynamic models of unified power flow controller for power system studies", IEEE Transactions on Power System, vol. 11, no. 4, pp. 1937-1950, 1996.

[17] H.F. Wang, "A unified model for the analysis of FACTS devices in damping power system oscillations –Part III: unified power flow controller', IEEE Transaction on Power Delivery, Vol. 15, No. 3, pp. 978–983, 2000.

[18] H.F. Wang, M. Jazaeri, Y.J. Cao, "Analysis of control conflict between UPFC multiple control functions and their interaction indicator", International Journal of Control, Automation, and Systems, Vol. 3, No. 2(special edition) , , pp. 315-321, 2005.

[19] K. Madhuri, M.V. Srikant, "Modeling and analysis of power flow controller in the presence of power system stabilizer for a multi-machine system", International Journal of Engineering Research & Technology (IJERT), Vol. 1, No. 6, pp. 1-7, 2012.

[20] M. Eslami, H. Shareef, M.R. Taha, M. Khajezadeh," Adaptive particle swarm optimization for simultaneous design of UPFC damping controllers", ELSEVIER Electrical Power and Energy Systems, Vol. 57, pp. 116-128, 2014.

[21] J. Fletcher, J. Yang, "Introduction to the Doubly-Fed Induction Generator for Wind Power Applications", D. A. Ng, Ed., InTech, pp. 259-279, 2010.

[22] H. *Jiang*, H. Liu, L. Wu, Y. Li, "*Comparisons* on State Space Models of Doubly Fed Induction Generators (*DFIG*) for Power System Research", State Grid Jibei Electric Power Research Institute. Beijing, China. IEEE PES Asia-Pacific Power and Energy Conference - Xi'an – China, 2016. DOI: 10.1109/APPEEC.2016.7779624.

[23] P. Kundur, "Power System Stability and Control", Electric Power Research Institute, Power System Engineering Series, McGraw-Hill, New York, 1994.

[24] W. Du, X. Chen, H.F. Wang, "Impact of dynamic interactions introduced by the DFIGs on power system electromechanical oscillation modes", IEEE, 0885-8950 (c) , 2016.

[25] W. Du, J. Bi, C. Ly, T. Littler, "Damping torque analysis of power systems with DFIGs for wind power generation", IET Proceedings on Renewable Power Generation, on-line early view, 2016.

[26] Illinois Center for a Smarter Electric Grid(ICSEG), "IEEE 39-Bus system".

[27] S. Q. Bu, X. Zhang, S. W. Xia, Y. Xu, B. Zhou, X. Lu , "Reducing model complexity of DFIG-based wind turbines to improve the efficiency of power system stability analysis", 9th International Conference on Applied Energy, ICAE2017, 21-24 August 2017, Cardiff, UK, Elsevier Energy Procedia, no. 142 .pp. 971-976, 2017.